

Mode Switching for MIMO Communication Based on Delay and Channel Quantization

Jun Zhang, Jeffrey G. Andrews, and Robert W. Heath Jr.*

Abstract

This paper proposes an adaptive multiple-input multiple-output (MIMO) transmission algorithm using imperfect channel state information at the transmitter. The approach switches between single-user and multi-user MIMO modes to improve the spectral efficiency, based on the average signal-to-noise ratio (SNR), the amount of delay, and the channel quantization codebook size. The achievable ergodic rates for both single-user and multi-user MIMO transmissions with different kinds of channel information are derived, which are used to calculate mode switching points. It is shown that single-user MIMO is relatively robust to imperfect channel information, while multi-user MIMO with zero-forcing precoding loses spatial multiplexing gain with a fixed delay or fixed codebook size. With imperfect channel information, as SNR increases, there are two mode switching points. The single-user mode is selected in both low and high SNR regimes, due to array gain and its robustness to the channel information error, respectively. The operating regions for single-user and multi-user modes with different delays and codebook sizes are determined, which can be used to select the preferred mode. It is shown that the multi-user mode may never be activated when the delay is large or the codebook size is small.

Index Terms

Multi-user MIMO, adaptive transmission, mode switching, imperfect channel state information at the transmitter (CSIT), zero-forcing precoding.

I. INTRODUCTION

Multiple-input multiple-output (MIMO) transmission is a promising technique for higher data rate wireless communications [1], [2]. Over the last decade, the point-to-point MIMO link (SU-MIMO) has

J. Zhang, J. G. Andrews, and R. W. Heath Jr. are with the Wireless Networking and Communications Group, Department of Electrical and Computer Engineering, The University of Texas at Austin, 1 University Station C0803, Austin, TX 78712-0240. Email: {jzhang2, jandrews, rheath}@ece.utexas.edu. This work has been supported by AT&T Labs, Inc.

been extensively researched and has transited from a theoretical concept to a practical technique. Due to space and complexity constraints, however, current mobile terminals only have one or two antennas, which limits the performance of the SU-MIMO link. Multi-user MIMO (MU-MIMO) provides the opportunity to overcome such a limitation by communicating with multiple mobiles simultaneously. It effectively increases the number of equivalent spatial channels and provides spatial multiplexing gain proportional to the number of transmit antennas at the base station. In addition, MU-MIMO has higher immunity to propagation limitations faced by SU-MIMO, such as channel rank loss and antenna correlation [3].

There are many technical challenges that must be overcome to exploit the full benefits of MU-MIMO. A major one is the requirement of channel state information (CSI) at the base station, which is difficult especially for the downlink/broadcast channel. Limited feedback [4]–[9], where quantized channel information is provided to the transmitter via a low-rate feedback channel, is one solution to this problem. Besides quantization, there are other imperfections in the available CSI at the base station, such as estimation error and feedback delay. Cumulatively, such imperfections will greatly degrade the performance of MU-MIMO [10]. With imperfect CSI, it is not clear whether—or more to the point, when—MU-MIMO can outperform SU-MIMO. In this paper, we propose to switch between SU and MU-MIMO modes based on the achievable rate of each technique with practical receiver assumptions.

A. Related Work

SU-MIMO communication has been well studied. With full CSI at the receiver (CSIR), the capacity of SU-MIMO grows linearly with the minimum number of transmit and receive antennas in the Rayleigh fading channel even with only channel distribution information at the transmitter [1]. Partial or full CSI at the transmitter (CSIT) can improve performance and reduce complexity. Recently, limited feedback techniques have been developed to exploit this performance gain for different transmission techniques [11]–[14]. With estimation errors at both the transmitter and receiver, the capacity bounds and optimal power allocation strategies for SU-MIMO were derived in [15].

For the MIMO broadcast channel, it has been shown that dirty-paper coding (DPC) [16] is optimal [17]–[20], but in practice it is difficult to implement. Therefore, low-complexity transmission techniques that are able to approach the optimal performance are required. Zero-forcing (ZF) and block diagonalization (BD)¹ are linear precoding techniques [21]–[23] that provide each user an interference-free channel.

¹Both ZF and BD are designed with the same criterion, i.e. to completely precancel inter-user interference at the transmitter. The difference is that ZF has a diagonal effective channel whereas BD has a block diagonal effective channel. In this paper, we denote such a precoder as *ZF* when $N_r = 1$ and as *BD* when $N_r > 1$.

While they enjoy low complexity and preserve the conventional single-user detector at mobiles, ZF and BD with perfect CSI can also achieve a significant part of the ergodic sum capacity of DPC [24], [25].

To acquire CSIT, practical limited feedback techniques for MU-MIMO have also been developed. To obtain the full spatial multiplexing gain for ZF and BD systems, it was shown in [4], [8] that the quantization codebook size needs to increase linearly with SNR (in dB). Zero-forcing DPC and channel inversion systems with limited feedback were studied in [7], where a sum rate ceiling due to a fixed codebook size was derived for both schemes. In [5], it was shown that to exploit multiuser diversity for the ZF system, both channel direction and information about signal-to-interference-plus-noise ratio (SINR) need to be fed back to the transmitter. More recently, a comprehensive study of ZF MU-MIMO downlink with channel estimation and feedback was done in [6], which concluded that very significant downlink throughput is achievable with efficient CSI feedback.

Although previous studies show that the spatial multiplexing gain of MU-MIMO can be achieved with limited feedback, it requires the codebook size to increase with SNR, which is challenging in practice. In addition, even if such a requirement is satisfied, there is an inevitable rate loss due to such imperfect CSIT. In this paper, we consider both CSI delay and channel quantization, and propose to switch between SU and MU modes based on the achievable rates.

B. Contributions

The main contributions of this paper are as follows.

- **SU vs. MU Analysis.** We investigate the impact of imperfect CSIT due to delay and channel quantization. We show that the SU mode is more robust to imperfect CSIT, while MU-MIMO suffers severe performance degradation due to residual inter-user interference and loses spatial multiplexing gain with a fixed delay or codebook size.
- **Mode Switching Algorithm.** Mode switching between SU and MU modes is proposed based on ergodic sum rate as a function of the average SNR, normalized Doppler frequency, and the quantization codebook size. Tight closed-form bounds/approximations give the mode switching points.
- **Operating Regions.** The *operating regions* for SU and MU modes are determined. With a fixed delay and codebook size, if the MU mode is possible at all, there are two mode switching points, with the SU mode preferred in both low and high SNR regimes. When delay is large, or the codebook size is small, the MU mode may never be activated.
- **Illustrative Examples.** We compare SU vs. MU for the practical cases of $N_t = 4$, $N_r = 1$ or 2. We see that BD is more robust to imperfect CSIT than ZF, but the operating region of BD is much smaller

than that of ZF. For $N_r = 2$, the downlink will operate in the SU mode for most of the scenarios with delay and quantization.

The rest of the paper is organized as follows. The system model and some assumptions are presented in Section II. In Section III, the SU and MU-MIMO systems with $N_r = 1$ are investigated, with perfect CSIT, with delay for TDD system, and with both delay and quantization for FDD system. In Section IV, the situation with $N_r > 1$ is studied. Conclusions are drawn in Section V.

II. SYSTEM MODEL

TABLE I
SYSTEM PARAMETERS

Symbol	Description
N_t	number of transmit antennas at the base station
N_r	number of receive antennas at each mobile
U	number of mobile users
B	number of feedback bits
L	quantization codebook size, $L = 2^B$
γ	average SNR
n	time index
D	CSI delay in the number of symbols
T_s	the length of each symbol
τ	the length of delay, $\tau = T_s D$
f_d	the Doppler frequency

We consider a MIMO downlink system, where the transmitter (base station) has N_t antennas and each mobile user has N_r antennas. The system parameters are listed in Table I. During each transmission period, the transmitter sends symbols to one (SU-MIMO mode) or multiple (MU-MIMO mode) users. The received signal at the u -th user at time n is given as²

$$\mathbf{y}_u[n] = \mathbf{H}_u[n] \mathbf{T}[n] \mathbf{x}[n] + \mathbf{z}_u[n], \quad (1)$$

²In this paper, we use uppercase boldface letters for matrices (\mathbf{X}) and lowercase boldface for vectors (\mathbf{x}). $\mathbb{E}[\cdot]$ is the expectation operator. The conjugate transpose of a matrix \mathbf{X} (vector \mathbf{x}) is \mathbf{X}^* (\mathbf{x}^*). Similarly, \mathbf{X}^\dagger denotes the pseudo-inverse, $\tilde{\mathbf{x}}$ denotes the normalized vector of \mathbf{x} , i.e. $\tilde{\mathbf{x}} = \frac{\mathbf{x}}{\|\mathbf{x}\|}$, and $\hat{\mathbf{x}}$ denotes the quantized vector of $\tilde{\mathbf{x}}$.

where $\mathbf{H}_u[n]$ is the $N_r \times N_t$ channel matrix from the transmitter to the u -th user, and $\mathbf{z}_u[n]$ is the normalized complex Gaussian noise vector with entries distributed according to $\mathcal{CN}(0, 1)$. For the SU mode, $\mathbf{x}[n]$ is the transmit signal for the u -th user, and $\mathbf{T}[n]$ is the transmit precoder for the u -th user. For the MU mode, $\mathbf{x}[n]$ is the aggregated signal, $\mathbf{x}[n] = [\mathbf{x}_1^*[n], \mathbf{x}_2^*[n], \dots, \mathbf{x}_U^*[n]]^*$, and $\mathbf{T}[n]$ is the aggregated precoding matrix, $\mathbf{T}[n] = [\mathbf{T}_1[n], \mathbf{T}_2[n], \dots, \mathbf{T}_U[n]]$. The transmit power constraint is $\mathbb{E}\{\mathbf{x}^*[n]\mathbf{x}[n]\} = \gamma$. As the noise is normalized, γ is also the value of the average SNR.

To assist the analysis, we assume that the channel $\mathbf{H}_u[n]$ is well modeled as a spatially white Gaussian channel, with entries $h_{i,j}[n] \sim \mathcal{CN}(0, 1)$. The results will be different for different channel models. For example, a limited feedback system with line of sight MIMO channel requires fewer feedback bits compared to the Rayleigh channel [26]. The investigation of other channel models is left to future work.

As the objective in this paper is to study the impact of imperfect CSIT, we assume perfect CSIR and the transmitter acts as if the CSIT is perfect. We study the following three CSIT scenarios.

- 1) *Perfect CSIT*: this is the baseline case where the transmitter has perfect CSI.
- 2) *TDD System*: for a TDD system, the transmitter can estimate the CSI through channel reciprocity. We assume such estimation is perfect. There will be delay in the available CSIT, however, due to propagation/processing/protocol.
- 3) *FDD System*: the receiver quantizes the CSI and feeds back to the transmitter through a dedicated low-rate feedback channel, so there are both CSI delay and channel quantization errors.

For MU-MIMO, we fix the number of users as $UN_r = N_t$, and do not consider user selection, as the main focus in this paper is spatial multiplexing gain rather than multiuser diversity gain.

A. CSI Delay Model

We consider a time-varying channel, where the channel stays constant for a symbol duration and changes from symbol to symbol according to a stationary correlation model. There is a delay of D symbols in the available CSIT. The current channel $\mathbf{H}[n]$ and its delayed version $\mathbf{H}[n - D]$ are jointly Gaussian with zero mean and are related in the following manner

$$\mathbf{H}[n] = \rho\mathbf{H}[n - D] + \mathbf{E}[n], \quad (2)$$

where $\mathbf{E}[n]$ is the channel error matrix, with i.i.d. entries $e_{i,j}[n] \sim \mathcal{CN}(0, \epsilon_e^2)$, and it is uncorrelated with $\mathbf{H}[n - D]$. For the numerical analysis, the classical Clarke's isotropic scattering model will be used as an example, for which the correlation coefficient is $\rho(D) = J_0(2\pi f_d D T_s)$ with Doppler spread f_d [27], where $J_0(\cdot)$ is the zero-th order Bessel function of the first kind, and $\epsilon_e^2(D) = 1 - \rho^2(D)$. Therefore,

both $\rho(D)$ and $\epsilon_e(D)$ are determined by the normalized Doppler frequency $f_d DT_s$. In the following, we will denote them as ρ and ϵ_e for simplicity.

This is a noiseless delayed feedback model used in [11], [28]. This model was also used to study the impact of feedback delay on the performance of closed-loop transmit diversity in [29] and the system capacity and BER of point-to-point MIMO link in [30]. Note that this model can also be used to model the estimation or prediction error [15], [31], so the results in this paper can be extended to these related systems.

B. Channel Quantization

For FDD systems, limited feedback techniques can provide partial CSIT through a dedicated feedback channel from the receiver to the transmitter. The channel information is fed back using a quantization codebook known at both the transmitter and receiver. Channel direction information is fed back for the precoder design, which is discussed in this section. The received SINR is assumed to be known perfectly to determine the transmit rate.

For $N_r = 1$, the quantization is chosen from a codebook of unit norm vectors of size $L = 2^B$. Each user uses a different codebook to avoid the same quantization vector. The codebook for user u is $\mathcal{C}_u = \{\mathbf{c}_{u,1}, \mathbf{c}_{u,2}, \dots, \mathbf{c}_{u,L}\}$. Each user quantizes its channel to the closest codeword, where closeness is measured by the inner product. Therefore, the index of channel for user u is

$$I_u = \arg \max_{1 \leq \ell \leq L} |\tilde{\mathbf{h}}_u^* \mathbf{c}_{u,\ell}|. \quad (3)$$

The transmitter has the quantized channel information $\hat{\mathbf{h}}_u = \mathbf{c}_{u,I_u}$. Random vector quantization (RVQ) [32] is used to facilitate the analysis, where each quantization vector is independently chosen from the isotropic distribution on the N_t -dimensional unit sphere.

The squared angular distortion is defined as $\sin^2(\angle(\tilde{\mathbf{h}}_u, \hat{\mathbf{h}}_u)) = 1 - |\tilde{\mathbf{h}}_u^* \hat{\mathbf{h}}_u|^2$. It was shown in [4] that the expectation of this quantity for i.i.d. Rayleigh fading is given by

$$\mathbb{E} \left[\sin^2 \left(\angle \left(\tilde{\mathbf{h}}_u, \hat{\mathbf{h}}_u \right) \right) \right] = 2^B \cdot \beta \left(2^B, \frac{N_t}{N_t - 1} \right), \quad (4)$$

where $\beta(\cdot)$ is the beta function. It can be tightly bounded as

$$\frac{N_t - 1}{N_t} 2^{-\frac{B}{N_t - 1}} \leq \mathbb{E} \left[\sin^2 \left(\angle \left(\tilde{\mathbf{h}}_u, \hat{\mathbf{h}}_u \right) \right) \right] \leq 2^{-\frac{B}{N_t - 1}}. \quad (5)$$

For $N_r > 1$, the quantization codebook \mathcal{C}_u for user u consists of 2^B matrices that satisfy $\mathbf{C}_\ell \mathbf{C}_\ell^* = \mathbf{I}_{N_r}$, $\forall \mathbf{C}_\ell \in \mathcal{C}_u$. The index of the quantized channel is chosen as

$$I_u = \arg \min_{1 \leq \ell \leq L} d^2(\mathbf{H}_u, \mathbf{C}_{u,\ell}). \quad (6)$$

The *chordal distance* is used as the distance metric [33]. The quantization distortion is defined as

$$\bar{D} = \mathbb{E} \left[\min_{\mathbf{C} \in \mathcal{C}_u} d^2(\mathbf{H}_u, \mathbf{C}) \right]. \quad (7)$$

With RVQ, it was shown in [34] that

$$\bar{D} \leq \frac{\Gamma\left(\frac{1}{T}\right)}{T} (C_{N_t N_r})^{-\frac{1}{T}} 2^{-\frac{B}{T}} + N_r \exp \left[- (2^B C_{N_t N_r})^{1-a} \right], \quad (8)$$

where $T = N_r(N_t - N_r)$ and $a \in (0, 1)$ is a real number between 0 and 1 chosen such that $(2^B C_{N_r N_t}) \leq 1$, with $C_{N_r N_t} = \frac{1}{T!} \prod_{i=1}^{N_r} \frac{(N_t - i)!}{(N_r - i)!}$.

C. Mode Switching

With imperfect CSIT, it is not clear whether and when the MU-MIMO system has a higher throughput than the SU-MIMO system. If the transmitter is able to estimate the achievable rates for both systems, it can adaptively activate the mode that provides a higher rate through SU/MU mode switching.

The channel correlation coefficient ρ , which captures the CSI delay effect, usually varies slowly. The codebook size, which determines the quality of the channel direction information fed back from the mobiles, is normally fixed for a given system. Therefore, it is reasonable to assume that the transmitter has knowledge of both delay and channel quantization. We will derive easy-to-evaluate bounds/approximations for the achievable ergodic rates for both SU and MU systems based on this information. The mode achieving a higher ergodic rate is activated, and then the transmitter informs either one (SU mode) or multiple (MU mode) active users. The active users feed back channel direction information, based on which the transmitter designs precoders. To get the received SINR, the transmitter sends pilot symbols, from which the active users estimate the received SINRs and feed back them to the transmitter. Then the data transmission starts.

III. BEAMFORMING VS. ZERO-FORCING ($N_r = 1$)

In this section, we derive the achievable rates for BF and ZF systems with $N_r = 1$ and different CSIT assumptions. With imperfect CSIT, for the BF system, we first calculate the average received SNR, and then apply the Jensen's inequality to get an upper bound for the achievable rate; for the ZF system, we analyze the noise plus residual interference, and get a lower bound for the achievable rate by approximating the interference as white Gaussian noise. The mode switching points are then calculated based on these bounds.

A. Perfect CSIT

1) *Beamforming*: With perfect CSIT, the BF vector is $\mathbf{t}[n] = \tilde{\mathbf{h}}[n]$. The average received SNR is

$$\overline{\text{SNR}}_{BF} = \mathbb{E} \{ \gamma |\mathbf{h}^*[n] \mathbf{t}[n]|^2 \} = \mathbb{E} \{ \gamma \|\mathbf{h}[n]\|^2 \} = \gamma N_t. \quad (9)$$

It achieves an array gain³ of N_t . The achievable rate of this system is the same as that of a maximal ratio combining diversity system, given by [36]

$$R_{BF}(\gamma) = \mathbb{E} [\log_2 (1 + \gamma \|\mathbf{h}[n]\|^2)] = \log_2(e) e^{1/\gamma} \sum_{k=0}^{N_t-1} \frac{\Gamma(-k, 1/\gamma)}{\gamma^k}, \quad (10)$$

where $\Gamma(\cdot, \cdot)$ is the complementary incomplete gamma function defined as $\Gamma(\alpha, x) = \int_x^\infty t^{\alpha-1} e^{-t} dt$.

2) *Zero-Forcing*: ZF is a linear precoding technique precanceling inter-user interference at the transmitter. With precoding vectors $\mathbf{t}_u[n], u = 1, 2, \dots, U$, assuming equal power allocation, the received SINR for the u -th user is given as

$$\text{SINR}_{ZF,u} = \frac{\frac{\gamma}{U} |\mathbf{h}_u^*[n] \mathbf{t}_u[n]|^2}{1 + \frac{\gamma}{U} \sum_{u' \neq u} |\mathbf{h}_{u'}^*[n] \mathbf{t}_{u'}[n]|^2}.$$

With perfect CSIT, this quantity can be calculated at the transmitter, while with imperfect CSIT, it can be estimated at the receiver and fed back to the transmitter given knowledge of $\mathbf{t}_u[n]$.

Denote $\tilde{\mathbf{H}}[n] = [\tilde{\mathbf{h}}_1[n], \tilde{\mathbf{h}}_2[n], \dots, \tilde{\mathbf{h}}_U[n]]^*$. With perfect CSIT, the ZF precoding vectors are determined from the pseudo-inverse of $\tilde{\mathbf{H}}[n]$, as $\mathbf{W}[n] = \tilde{\mathbf{H}}^\dagger[n] = \tilde{\mathbf{H}}^*[n] (\tilde{\mathbf{H}}[n] \tilde{\mathbf{H}}^*[n])^{-1}$. The precoding vector for the u -th user is obtained by normalizing the u -th column of $\mathbf{W}[n]$. Therefore, $\mathbf{h}_u^*[n] \mathbf{t}_{u'}[n] = 0, \forall u \neq u'$, i.e. there is no inter-user interference. The received SINR for the u -th user becomes

$$\text{SINR}_{ZF,u} = \frac{\gamma}{U} |\mathbf{h}_u^*[n] \mathbf{t}_u[n]|^2. \quad (11)$$

As $\mathbf{t}_u[n]$ is independent of $\mathbf{h}_u[n]$, and $\|\mathbf{t}_u[n]\|^2 = 1$, the effective channel for the u -th user is a SISO Rayleigh fading channel. Therefore, the achievable sum rate for the ZF system is given by

$$R_{ZF}(\gamma) = \sum_{u=1}^U \mathbb{E} [\log_2 (1 + \text{SINR}_{ZF,u})]. \quad (12)$$

Each term on the right hand side of (12) is the ergodic capacity of a SISO system in Rayleigh fading, given in [36] as

$$R_{ZF,u} = \mathbb{E} [\log_2 (1 + \text{SINR}_{ZF,u})] = \log_2(e) e^{U/\gamma} E_1(U/\gamma), \quad (13)$$

³The array gain is defined as the increase in the average combined SNR over the average SNR on each branch [35].

where $E_1(\cdot)$ is the exponential-integral function of the first order, $E_1(x) = \int_1^\infty \frac{e^{-xt}}{t} dt$. With i.i.d. channels for all the users,

$$R_{ZF}(\gamma) = UR_{ZF,u} = U \log_2(e) e^{U/\gamma} E_1(U/\gamma), \quad (14)$$

which shows a spatial multiplexing gain of U .

3) *Mode Switching Point*: As the array gain dominates the performance at low SINR while the spatial multiplexing gain dominates at high SINR, the system throughput can be improved by switching between SU and MU modes based on the average SNR. The mode switching point is computed by solving $R_{BF}(\gamma) = R_{ZF}(\gamma)$. For $N_t = 4$, it is calculated to be $\gamma^* = 7.77$ dB.

Fig. 1 depicts the numerical results for this baseline case for $N_t = 4$. It is shown that the system should operate in the *SU BF region* for the array gain when $\gamma \leq \gamma^*$ and in the *MU ZF region* for the spatial multiplexing gain when $\gamma > \gamma^*$. There is only one switching point. In the following sections, we will show how the operating regions change if there are delay and channel quantization.

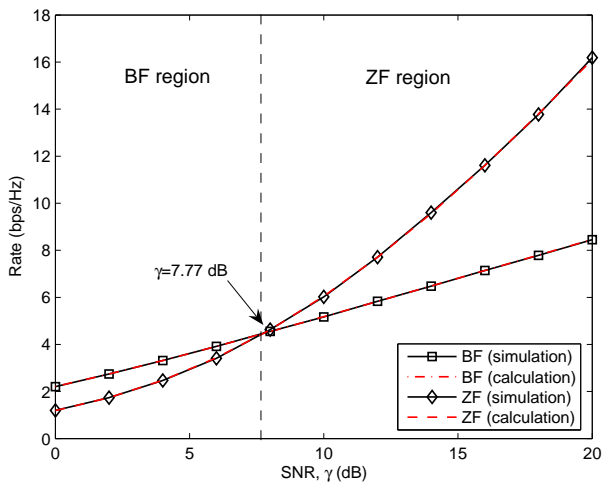


Fig. 1. Switching point between BF and ZF modes with perfect CSIT, $N_t = 4$.

B. TDD System–CSI Delay

1) *Beamforming*: With delay, the BF vector is $\mathbf{t}^{(D)}[n] = \tilde{\mathbf{h}}[n - D]$. The average received SNR is given by the following theorem.

Theorem 1: The average received SNR for a BF system with delayed CSIT is given by

$$\overline{\text{SNR}}_{BF}^{(D)} = \gamma (\rho^2 N_t + \epsilon_e^2). \quad (15)$$

Proof: See Appendix A. ■

With Jensen's inequality, an upper bound for the achievable rate is given as

$$R_{BF}^{(D)} = \mathbb{E} \left[\log_2 \left(1 + \gamma \left| \mathbf{h}^*[n] \mathbf{t}^{(D)}[n] \right|^2 \right) \right] \quad (16)$$

$$\leq \log_2 \left[1 + \overline{\text{SNR}}_{BF}^{(D)} \right]. \quad (17)$$

Remark 1: A fixed delay introduces a constant factor to the average SNR, which decreases as ρ decreases ($f_d \tau$ increases) or N_t increases. At high SNR, the performance degradation is a constant rate loss, which is $\log_2 \left(\rho^2 + \frac{\epsilon_e^2}{N_t} \right)$, independent of γ .

2) *Zero-forcing:* With delay, the ZF precoding vectors are designed based on the outdated CSIT, which only achieve $\tilde{\mathbf{h}}_u^*[n-D] \mathbf{t}_{u'}^{(D)}[n] = 0, \forall u \neq u'$. So there will be mutual interference, and

$$\mathbf{h}_u^*[n] \mathbf{t}_{u'}^{(D)}[n] = (\rho \mathbf{h}_u[n-D] + \mathbf{e}_u[n])^* \mathbf{t}_{u'}^{(D)}[n] = \mathbf{e}_u^*[n] \mathbf{t}_{u'}^{(D)}[n], \forall u \neq u'.$$

Therefore, the received SINR for the u -th user is

$$\text{SINR}_{ZF,u}^{(D)} = \frac{\frac{\gamma}{U} |\mathbf{h}_u^*[n] \mathbf{t}_u^{(D)}[n]|^2}{1 + \frac{\gamma}{U} \sum_{u' \neq u} |\mathbf{e}_u^*[n] \mathbf{t}_{u'}^{(D)}[n]|^2}. \quad (18)$$

As $\mathbf{t}_u^{(D)}[n]$ is in the nullspace of $\tilde{\mathbf{h}}_{u'}[n-D] \forall u' \neq u$, it is isotropically distributed in \mathbb{C}^{N_t} and independent of $\tilde{\mathbf{h}}_u[n-D]$ as well as $\tilde{\mathbf{h}}_u[n]$, so $|\mathbf{h}_u^*[n] \mathbf{t}_u^{(D)}[n]|^2 \sim |\mathbf{h}_u^*[n] \mathbf{t}_u[n]|^2$. The performance degradation due to CSI delay is brought by the denominator of (18), which is the noise-plus-interference term. Such degradation is described in the following theorem.

Theorem 2: For the ZF system with CSI delay, the average noise plus interference for the u -th user is

$$\Delta_{ZF,u}^{(D)} = 1 + (U-1) \frac{\gamma}{U} \epsilon_{e,u}^2. \quad (19)$$

Proof: The proof is similar to *Theorem 1*, from the independence of $\mathbf{e}_u[n]$ and $\mathbf{t}_{u'}^{(D)}[n]$ ■

Remark 2: We see that the average residual interference for a given user consists of three parts: 1) *The amount of delay for this user*⁴, which is reflected from $\epsilon_{e,u}^2$. The user with a larger delay suffers a higher residual interference. 2) *The transmit power of the other active users*, $\frac{\gamma}{U}$. As the transmit power increases, the system becomes interference-limited. It is possible to improve performance through power allocation, which is left to future work. 3) *The number of interferers*, $U-1$. The more users the system supports, the higher the mutual interference.

⁴For illustrative examples in this paper, we assume all the users have the same CSI delay, but as the statement made here, the analysis results are general.

TABLE II
PROPERTIES OF VIRTUAL INTERFERING USERS (VIU)

	TDD System		FDD System	
	Number of VIU	Equivalent SNR	Number of VIU	Equivalent SNR
ZF ($N_r = 1$)	$N_t - 1$	$\frac{\gamma}{N_t} \epsilon_{e,u}^2$	$N_t - 1$	$\frac{\gamma}{N_t} (\rho_u^2 \frac{N_t}{N_t-1} \cdot 2^{-\frac{B}{N_t-1}} + \epsilon_{e,u}^2)$
BD ($N_r > 1$)	$N_t - N_r$	$\frac{\gamma}{N_t} \epsilon_{e,u}^2$	$N_t - N_r$	$\frac{\gamma}{N_t} (\rho_u^2 \frac{N_t}{N_t-N_r} \cdot \frac{D}{N_r} + \epsilon_{e,u}^2)$

From this remark, the interference term, $\frac{\gamma}{U}(U-1)\epsilon_{e,u}^2$, equivalently comes from $U-1$ *virtual interfering users*, each with equivalent SNR as $\frac{\gamma}{U}\epsilon_{e,u}^2$. With a high γ and fixed $\epsilon_{e,u}$, the system is interference-limited and can not achieve full spatial multiplexing gain. Therefore, to keep a constant rate loss, i.e. to sustain the spatial multiplexing gain, the CSI delay should be reduced with the increase of SNR, which is usually not possible in practice. The properties of the virtual interfering users (VIU) for different MU systems are compared in Table II.

For ZF with imperfect CSI, upper and lower bounds for the achievable rate are given in [6]. The genie-aided upper bound⁵ is given by

$$R_{ZF}^{(D)} \leq \sum_{u=1}^U \mathbb{E} \left[\log_2 \left(1 + \text{SINR}_{ZF,u}^{(D)} \right) \right]. \quad (20)$$

An easy-to-evaluate lower bound is

$$R_{ZF}^{(D)} \geq R_{ZF} - \sum_{u=1}^U \log_2 \Delta_{ZF,u}^{(D)}, \quad (21)$$

where R_{ZF} is the achievable rate with perfect CSIT, given in (14).

We assume the mobile users can perfectly estimate the noise and interference and feed back it to the transmitter, so the upper bound is chosen as the performance metric, as in [4], [5], [7]. However, it is difficult to calculate. In addition, the lower bound (21) is loose. We will use the following lower bound to derive the mode switching point:

$$R_{ZF}^{(D)} \geq \sum_{u=1}^U \mathbb{E} \left[\log_2 \left(1 + \frac{\text{SINR}_{ZF,u}}{\Delta_{ZF,u}^{(D)}} \right) \right] = \sum_{u=1}^U R_{ZF,u} \left(\frac{\gamma/U}{\Delta_{ZF,u}^{(D)}} \right), \quad (22)$$

where $\text{SINR}_{ZF,u}$ is the SINR of the u -th user with perfect CSIT, given in (11), $\Delta_{ZF,u}^{(D)}$ is the equivalent noise variance, as in *Theorem 2*, and $R_{ZF,u}(\cdot)$ is the achievable rate for the u -th user with perfect CSIT, given by (13). Effectively, this is to approximate the residual inter-user interference with uncorrelated

⁵This upper bound is achievable only when a genie provides users with perfect knowledge of all interference.

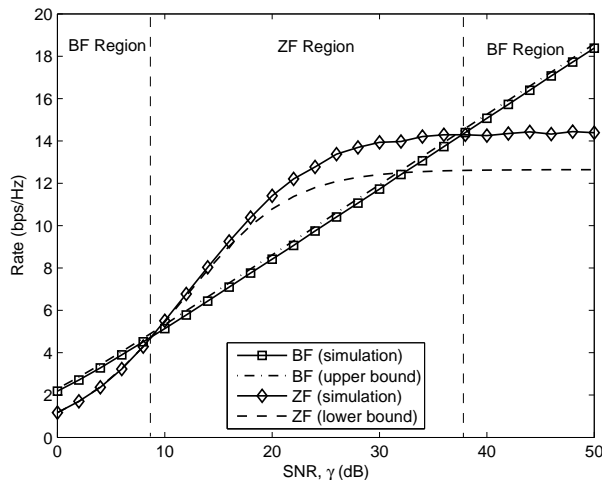


Fig. 2. Switching points between BF and ZF modes with CSI delay, $N_t = 4$, $f_c = 2$ GHz, $\tau = 0.001$ sec, and terminal speed is 20 km/hr.

Gaussian noise with the same variance. Therefore, it is a lower bound as Gaussian noise is the worst-case noise distribution. The same approach was taken in [37], [38].

3) *Mode Switching Point*: Equating right hand sides of (17) and (22), the approximation for the switching point γ^* can be calculated. Different from the system with perfect CSIT, there may be two switching points for the system with delay. These two points can be calculated by providing different initial values to the nonlinear equation solver, such as *fsolve* in MATLAB. If no solution is found, the SU mode is always active; if one solution is found, the SU mode is active at low SNR while the MU mode is active at high SNR, as shown in Fig. 1; if two solutions are found, the SU mode is active at both high and low SNR, while the MU mode is active at medium SNR.

An example of mode switching is shown in Fig. 2, with carrier frequency $f_c = 2$ GHz, CSI delay $\tau = 0.001$ second and the terminal speed $v = 20$ km/hr, which means $f_d\tau = 0.037$. The simulation results average over 10000 channel realizations, according to (16) and (20) for BF and ZF, respectively, and the upper and lower bounds follow (17) and (22). We see that with a fixed delay, the ZF system cannot attain full multiplexing gain, while the BF system only has a slight rate loss compared to the perfect CSIT case in Fig. 1. In contrast to the system with perfect CSIT, there are two switching points. The SU mode is preferred at low SNR due to its array gain and preferred at high SNR due to its robustness to the CSI delay. The prediction for the first switching point ($\gamma^* = 9.56$ dB) is accurate, while the prediction for the second switching point is conservative ($\gamma^* = 31.65$ dB), the reason for which is stated in the following

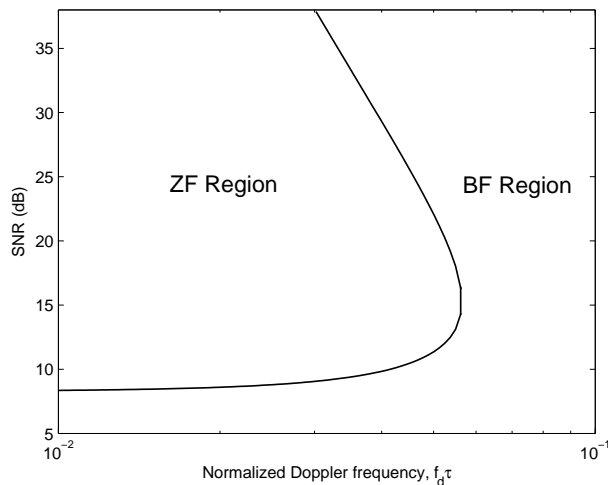


Fig. 3. Operating regions for BF and ZF with different CSI delays, $N_t = 4$.

remark.

Remark 3: Note that we use an upper bound for the BF system and a lower bound for the ZF system to get the switching point, which means we tend to favor the more robust BF system. This is a reasonable approach for practical design. In addition, from Fig. 2 we see that the bounds are tight at low SNR and can accurately predict the first switching point. This philosophy also applies in the next section.

Finding switching points requires solving a nonlinear equation, which does not have a closed-form solution and gives little insight. However, it is easy to evaluate numerically for different parameters, from which insights can be drawn. In Fig. 3, we plot the operating regions for both modes for different delays. We see that for the ZF mode to be active, $f_d\tau$ needs to be small and SNR needs to be high. Specifically, for $N_t = 4$, ZF is possible to be active only when $\text{SNR} > 8.35$ dB and $f_d\tau < 0.057$. For $f_d\tau < 0.057$, there are two mode switching points. The BF mode is active in both low and high SNR regimes.

C. FDD System–CSI Delay and Channel Quantization

1) *Beamforming:* First, if there is no delay and only channel quantization, the BF vector is based on the quantized feedback, $\mathbf{t}^{(Q)}[n] = \hat{\mathbf{h}}[n]$. The average received SNR is

$$\begin{aligned} \overline{\text{SNR}}_{BF}^{(Q)} &= \mathbb{E}[\gamma |\mathbf{h}^*[n] \hat{\mathbf{h}}[n]|^2] \\ &= \mathbb{E}[\gamma \|\mathbf{h}[n]\|^2 |\tilde{\mathbf{h}}^*[n] \hat{\mathbf{h}}[n]|^2] \\ &\stackrel{(a)}{\leq} \gamma N_t \left(1 - \frac{N_t - 1}{N_t} 2^{-\frac{B}{N_t - 1}} \right) \end{aligned}$$

$$= \overline{\text{SNR}}_{BF} \left(1 - \frac{N_t - 1}{N_t} 2^{-\frac{B}{N_t - 1}} \right), \quad (23)$$

where (a) follows the independence between $\|\mathbf{h}[n]\|^2$ and $|\tilde{\mathbf{h}}^*[n]\hat{\mathbf{h}}[n]|^2$, together with the result in (5). Similar to the CSI delay, the channel quantization adds a degradation factor on SNR. Based on this, together with the result for the delayed system in *Theorem 1*, the following theorem provides the average SNR for the system with both delay and quantization.

Theorem 3: The average received SNR for a BF system with channel quantization and CSI delay is

$$\overline{\text{SNR}}_{BF}^{(QD)} \leq \gamma N_t \left(\rho^2 \Delta_{BF}^{(Q)} + \Delta_{BF}^{(D)} \right) = \overline{\text{SNR}}_{BF} \Delta_{BF}^{(QD)}, \quad (24)$$

where $\Delta_{BF}^{(Q)}$ and $\Delta_{BF}^{(D)}$ are the degradations brought by channel quantization and feedback delay, respectively, given by

$$\Delta_{BF}^{(Q)} = 1 - \frac{N_t - 1}{N_t} 2^{-\frac{B}{N_t - 1}}, \quad \Delta_{BF}^{(D)} = \frac{\epsilon_c^2}{N_t}.$$

Proof: This theorem comes from the result (23) for the limited feedback system and *Theorem 1* for the delayed BF system. ■

An upper bound of the achievable rate for the BF system with both quantization and delay is

$$R_{BF}^{(QD)} = \mathbb{E} \left[\log_2 \left(1 + \gamma |\mathbf{h}^*[n] \mathbf{t}^{(QD)}[n]|^2 \right) \right] \quad (25)$$

$$\leq \log_2 \left[1 + \gamma N_t \left(\rho^2 \Delta_{BF}^{(Q)} + \Delta_{BF}^{(D)} \right) \right]. \quad (26)$$

Remark 4: The above results show the impact of the channel quantization and CSI delay on the performance of a BF system through $\Delta_{BF}^{(Q)}$ and $\Delta_{BF}^{(D)}$, respectively. Similar to the TDD system with delay, with a fixed B and fixed delay, the SNR degradation is a constant factor independent of γ . At high SNR, the imperfect CSIT introduces a constant rate loss $\log_2 \left(\rho^2 \Delta_{BF}^{(Q)} + \Delta_{BF}^{(D)} \right)$.

2) *Zero-Forcing:* If there is no delay, the precoding vectors for the ZF system with limited feedback are designed based on $\hat{\mathbf{h}}_1[n], \hat{\mathbf{h}}_2[n], \dots, \hat{\mathbf{h}}_U[n]$ to achieve $\hat{\mathbf{h}}_u^*[n] \mathbf{t}_{u'}^{(Q)}[n] = 0, \forall u \neq u'$. With random vector quantization, it is shown in [4] that the average noise plus interference for each user is

$$\Delta_{ZF,u}^{(Q)} = \mathbb{E} \left[1 + \frac{\gamma}{U} \sum_{u' \neq u} |\mathbf{h}_u^*[n] \mathbf{t}_{u'}^{(Q)}[n]|^2 \right] = 1 + 2^{-\frac{B}{N_t - 1}} \gamma. \quad (27)$$

With both channel quantization and CSI delay, precoding vectors are designed based on $\hat{\mathbf{h}}_1[n - D], \hat{\mathbf{h}}_2[n - D], \dots, \hat{\mathbf{h}}_U[n - D]$ as $\hat{\mathbf{h}}_u^*[n - D] \mathbf{t}_{u'}^{(QD)}[n] = 0, \forall u \neq u'$. The SINR is given as

$$\text{SINR}_{ZF,u}^{(QD)} = \frac{\frac{\gamma}{U} |\mathbf{h}_u^*[n] \mathbf{t}_u^{(QD)}[n]|^2}{1 + \frac{\gamma}{U} \sum_{u' \neq u} |\mathbf{h}_u^*[n] \mathbf{t}_{u'}^{(QD)}[n]|^2}. \quad (28)$$

Similar to (18), $|\mathbf{h}_u^*[n]\mathbf{t}_u^{(QD)}[n]|^2 \sim |\mathbf{h}_u^*[n]\mathbf{t}_u[n]|^2$. The average noise plus interference is given in the following theorem.

Theorem 4: The average noise plus interference for the u -th user of the ZF system with both channel quantization and CSI delay is

$$\Delta_{ZF,u}^{(QD)} = 1 + (U - 1) \frac{\gamma}{U} (\rho_u^2 \Delta_{ZF,u}^{(Q)} + \Delta_{ZF,u}^{(D)}), \quad (29)$$

where $\Delta_{ZF,u}^{(Q)}$ and $\Delta_{ZF,u}^{(D)}$ are the degradations brought by channel quantization and feedback delay, respectively, given by

$$\Delta_{ZF,u}^{(Q)} = \frac{U}{U-1} 2^{-\frac{B}{N_t-1}}, \quad \Delta_{ZF,u}^{(D)} = \epsilon_{e,u}^2.$$

Proof: See Appendix B. ■

Remark 5: *Theorem 4* shows the performance degradation due to both channel quantization and CSI delay through $\Delta_{ZF,u}^{(Q)}$ and $\Delta_{ZF,u}^{(D)}$, respectively. The same observations as in *Remark 2* can be made. In addition, $\Delta_{ZF,u}^{(QD)}$ increases as B decreases. There are $U - 1$ *virtual interfering users* with the equivalent SNR as $\frac{\gamma}{U} (\rho_u^2 \Delta_{ZF,u}^{(Q)} + \Delta_{ZF,u}^{(D)})$, which makes the system interference-limited with a fixed delay/codebook size.

For the achievable rate, similar to the TDD system, we get the genie-aided upper bound

$$R_{ZF}^{(QD)} \leq \sum_{u=1}^U \mathbb{E} \left[1 + \text{SINR}_{ZF,u}^{(QD)} \right], \quad (30)$$

and the lower bound

$$R_{ZF}^{(QD)} \geq \sum_{u=1}^U \mathbb{E} \left[\log_2 \left(1 + \frac{\text{SINR}_{ZF,u}}{\Delta_{ZF,u}^{(QD)}} \right) \right] = \sum_{u=1}^U R_{ZF,u} \left(\frac{\gamma}{U \Delta_{ZF,u}^{(QD)}} \right) \quad (31)$$

by approximating the residual interference as Gaussian noise.

3) *Mode Switching Point:* Equating right hand sides of (26) and (31), the mode switching point γ^* can be calculated. A numerical example is shown in Fig. 4. Totally 10000 channel realizations are simulated. The simulation results follow (25) and (30) for BF and ZF, respectively, while the bounds follow (26) and (31). Similar to the TDD system, there are two switching points. The lower bound for ZF is shown to be loose at high SNR, but it accurately predicts the first switching point. The operating regions are similar to that of the TDD system. The SU mode is active for both low and high SNR.

The switching point now depends on both delay and codebook size. In Fig. 5, the operating regions for both modes are plotted. There are analogies between two plots. Some key observations are as follows:

- For the delay plot Fig. 5(a), compared to Fig. 3, the ZF operating region shrinks, which is due to the quantization error. The smaller the codebook size, the smaller the operating region for the ZF mode.

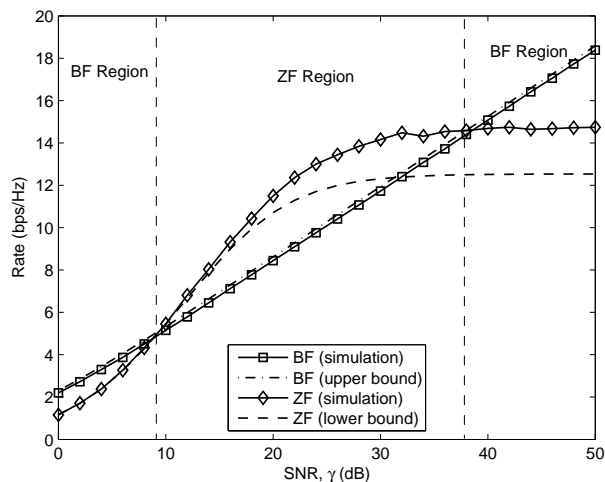
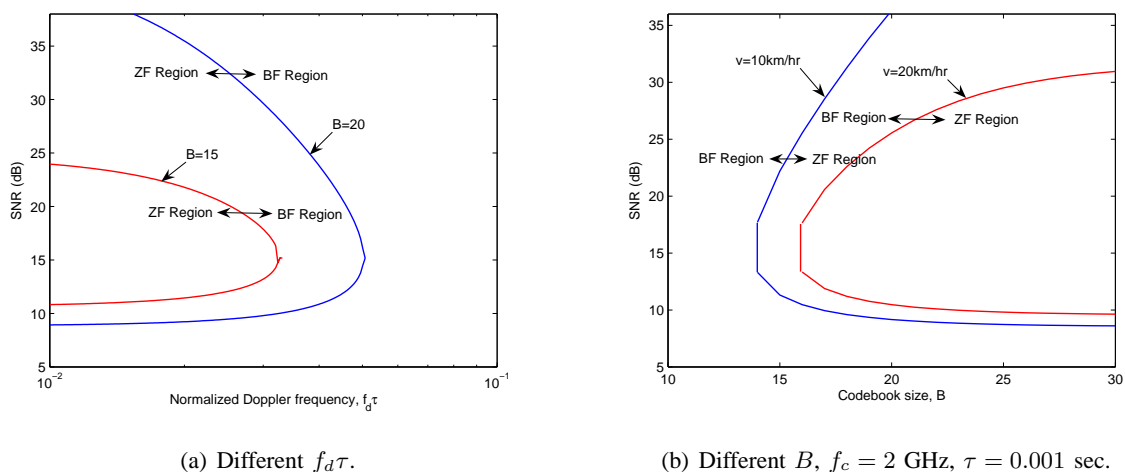


Fig. 4. Switch points between BF and ZF modes with both CSI delay and channel quantization, $B = 18$, $N_t = 4$, $f_c = 2$ GHz, $\tau = 0.001$ sec, $v = 10$ km/hr.



(a) Different $f_d \tau$.

(b) Different B , $f_c = 2$ GHz, $\tau = 0.001$ sec.

Fig. 5. Operating regions for BF and ZF with both CSI delay and quantization, $N_t = 4$.

- For the codebook size plot Fig. 5(b), as $f_d \tau$ increases (v increases), the ZF operating region shrinks. For the ZF mode to be active, we should have $B \geq 14$ and $B \geq 16$ for $v = 10$ km/hr and $v = 20$ km/hr, respectively, which means a large codebook size. Note that for BF we only need a small codebook size to get the near-optimal performance [14].

IV. SVD TRANSCEIVER VS. BLOCK DIAGONALIZATION ($N_r > 1$)

In this section, we consider the scenario with $N_r > 1$. We assume each user receives N_r streams. The SVD transceiver, with precoder and decoder derived from the singular value decomposition (SVD) of the channel matrix, is applied for the SU mode while BD precoding is applied for the MU mode. For ease of calculation, we will apply asymptotic results from random matrix theory [39] to analyze both systems, which have been shown to be accurate even for small N_r and N_t [40]. As shown in the last section, the SU mode is relatively robust to imperfect CSIT. Therefore, in this section we provide detail analysis for the BD system, while for the SVD system we will use the asymptotic result for the perfect CSIT case for all the scenarios, which serves as an upper bound with imperfect CSIT and is easy to calculate.

A. Perfect CSIT

1) *SVD Transceiver*: With perfect CSIT, the SVD transceiver is optimal for the point-to-point MIMO link [1]. Denote the SVD of the channel matrix as $\mathbf{H}[n] = \mathbf{U}[n]\mathbf{\Lambda}[n]\mathbf{V}^*[n]$. The precoding matrix is $\mathbf{V}[n]$ while the decoding matrix is $\mathbf{U}[n]$. The optimal input is $\mathbf{\Phi} = \mathbb{E}[\mathbf{x}[n]\mathbf{x}^*[n]] = \mathbf{V}[n]\mathbf{P}[n]\mathbf{V}^*[n]$, with power loading matrix $\mathbf{P}[n]$ obtained through water-filling power allocation.

The asymptotic results for such a system was presented in [41], as $N_t, N_r \rightarrow \infty$ with $\frac{N_t}{N_r} \rightarrow \beta$, which is valid only for a certain range of SNR due to the water-filling power allocation. Recall that the capacity gain of the MIMO system with full CSIT over that with channel distribution information at the transmitter (CDIT) comes from a power gain of $\frac{N_t}{N_r}$ for $N_t > N_r$, as with CSIT the transmit power can be focused on N_r non-zero eigenmodes [42]. To assist the analysis of mode switching, we approximate the capacity with perfect CSIT by the one with CDIT but with $\gamma\frac{N_t}{N_r}$ as the effective SNR.

With CDIT and perfect CSIR, the optimal input covariance for i.i.d. Rayleigh fading channel is $\mathbf{\Phi} = \frac{\gamma}{N_t}\mathbf{I}_{N_r}$ with Gaussian distribution [1]. The ergodic capacity for this system is then given by

$$C_{iso} = \mathbb{E} \left[\log \det \left(\mathbf{I}_{N_r} + \frac{\gamma}{N_t} \mathbf{H}[n] \mathbf{H}^*[n] \right) \right]. \quad (32)$$

The following theorem gives the asymptotic result for this capacity as $N_t, N_r \rightarrow \infty$ with $\frac{N_t}{N_r} \rightarrow \beta$.

Theorem 5 ([43], [44]): For a point-to-point MIMO link with CDIT and full CSIR, the asymptotic capacity per receive antenna is

$$\frac{C_{iso}(\beta, \gamma)}{N_r} = \log_2 \left[1 + \gamma - \mathcal{F} \left(\beta, \frac{\gamma}{\beta} \right) \right] + \beta \log_2 \left[1 + \frac{\gamma}{\beta} - \mathcal{F} \left(\beta, \frac{\gamma}{\beta} \right) \right] - \beta \frac{\log_2(e)}{\gamma} \mathcal{F} \left(\beta, \frac{\gamma}{\beta} \right) \quad (33)$$

with

$$\mathcal{F}(x, y) = \frac{1}{4} \left[\sqrt{1 + y(1 + \sqrt{x})^2} - \sqrt{1 + y(1 - \sqrt{x})^2} \right]^2.$$

Therefore, the ergodic capacity of the SVD system with perfect CSIT is approximated as

$$C_{SVD} \approx \mathbb{E} \left[\log \det \left(\mathbf{I}_{N_r} + \frac{\beta\gamma}{N_t} \mathbf{H}[n] \mathbf{H}^*[n] \right) \right] = \mathcal{C}_{iso}(\beta, \beta\gamma). \quad (34)$$

This is easy to calculate and valid for the whole SNR range. In addition, it will be shown later that this approximation is accurate.

2) *BD System*: With perfect CSIT and assuming the channels are sufficiently different, BD precoding achieves $\mathbf{H}_u[n] \mathbf{T}_{u'}[n] = \mathbf{0}$, $\forall u' \neq u$. To assist the analysis, $\mathbf{T}_u[n]$ is constrained to be a unitary matrix, i.e. $\mathbf{T}_u^*[n] \mathbf{T}_u[n] = \mathbf{I}_{N_r}$, which is consistent with the uniform power allocation assumed in this paper. In this way, user u sees an $N_r \times N_r$ effective point-to-point interference-free channel. Its received signal becomes

$$\mathbf{y}_u[n] = \mathbf{H}_u[n] \mathbf{T}_u[n] \mathbf{x}_u[n] + \mathbf{z}_u[n] = \mathbf{H}_{eff,u}[n] \mathbf{x}_u[n] + \mathbf{z}_u[n], \quad (35)$$

where $\mathbf{H}_{eff,u}[n] = \mathbf{H}_u[n] \mathbf{T}_u[n]$. As $\mathbf{T}_u[n]$ is a unitary matrix, which is independent of $\mathbf{H}_u[n]$, $\mathbf{H}_{eff,u}[n]$ is also a complex Gaussian matrix as $\mathbf{H}[n]$, i.e. $\mathbf{H}_{eff,u}[n] \sim \mathcal{CN}(\mathbf{0}_{N_r \times N_r}, N_r \mathbf{I}_{N_r})$.

Assuming the number of data streams for user u is equal to the number of receive antennas of user u , and with equal power allocation, the input covariance is $\Phi_{BD,u} = \frac{\gamma}{N_t} \mathbf{I}_{N_r}$ ⁶. The achievable ergodic rate for the u -th user is given by

$$R_{BD,u} = \mathbb{E} \left[\log_2 \det \left(\mathbf{I}_{N_r} + \frac{\gamma}{N_t} \mathbf{H}_{eff,u}[n] \mathbf{H}_{eff,u}^*[n] \right) \right], \quad (36)$$

which is similar to (32), but with an $N_r \times N_r$ effective channel. Therefore, the achievable rate for the BD system with perfect CSIT is given as

$$R_{BD} = \sum_{u=1}^U R_{BD,u} \approx U N_r \mathcal{C}_{iso}(1, \gamma/\beta). \quad (37)$$

The spatial multiplexing gain of BD is $U N_r$, compared to N_r for the SVD system.

3) *Mode Switching Point*: Equating (34) and (37), the approximation of the mode switching point for SU and MU modes can be calculated. Some numerical results are shown in Fig. 6. We see that the asymptotic approximation is good for SVD and is slightly loose for BD system at high SNR, due to the effective low-dimension 2×2 channels for BD users. However, it accurately predicts the switching point. With perfect CSIT, there is only one switching point. The SVD mode is active at low SNR due to its array gain; the BD mode is preferred at high SNR due to its enhanced spatial multiplexing gain. Compared to the results for $N_r = 1$ in Fig. 1, the switching point is a little higher. This is because the

⁶At high SNR, this performs closely to the system employing optimal water-filling, as power allocation mainly benefits at low SNR. This has been verified in [45].

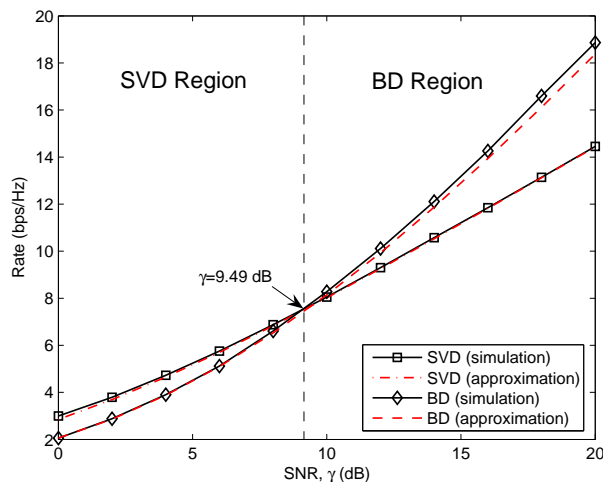


Fig. 6. Switching point between SVD and BD modes with perfect CSIT, $N_t = 4$, $N_r = 2$.

SVD system can provide spatial multiplexing gain in addition of the array gain while the BF system can only provide array gain.

B. TDD System–CSI Delay

1) *SVD Transceiver*: With CSI delay, the SVD transceiver based on the outdated channel cannot perfectly diagonalize the channel matrix. The receiver performs joint decoding rather than separate decoding which is only possible with perfect CSIT. Therefore, the achievable rate is

$$R_{SVD}^{(D)} = \mathbb{E} [\log \det (\mathbf{I}_{N_r} + \mathbf{H}[n]\Phi[n-D]\mathbf{H}^*[n])], \quad (38)$$

where $\Phi[n-D]$ is the input covariance based on the outdated CSIT. The receiver estimates this achievable rate based on the pilot symbol and feeds back it to the transmitter. This rate is difficult to calculate. From section III, the BF system is very robust to the CSI delay. We would expect it is also the case for the SVD system. Therefore, we will approximate (38) by (34) for the system with perfect CSIT, which will later be verified by numerical results.

2) *BD System*: With delayed CSIT, BD precoding matrices cannot perfectly cancel mutual interference, as they only achieve $\mathbf{H}_u[n-D]\mathbf{T}_{u'}^{(D)}[n] = \mathbf{0}$, $\forall u' \neq u$. The received signal for user u thus becomes

$$\mathbf{y}_u[n] = \mathbf{H}_{eff,u}[n]\mathbf{x}_u[n] + \mathbf{E}_u[n] \sum_{u' \neq u} \mathbf{T}_{u'}^{(D)}[n]\mathbf{x}_{u'}[n] + \mathbf{z}_u[n]. \quad (39)$$

Treating residual interference as noise, the achievable rate for the u -th user is given by

$$R_{BD,u}^{(D)} = \mathbb{E} \left[\log_2 \det \left(\mathbf{I}_{N_r} + \frac{\gamma}{N_t} \mathbf{H}_{eff,u}[n] \mathbf{H}_{eff,u}^*[n] \mathbf{R}_u^{-1}[n] \right) \right], \quad (40)$$

where $\mathbf{R}_u[n]$ is the interference-plus-noise covariance matrix, given by

$$\begin{aligned} \mathbf{R}_u[n] &= \mathbf{E}_u[n] \mathbb{E} \left[\sum_{u' \neq u} \mathbf{T}_{u'}^{(D)}[n] \mathbf{x}_{u'}[n] \mathbf{x}_{u'}^*[n] \mathbf{T}_{u'}^{(D)*}[n] \right] \mathbf{E}_u^*[n] + \mathbf{I}_{N_r} \\ &= \mathbf{E}_u[n] \left[\sum_{u' \neq u} \frac{\gamma}{N_t} \mathbf{T}_{u'}^{(D)}[n] \mathbf{T}_{u'}^{(D)*}[n] \right] \mathbf{E}_u^*[n] + \mathbf{I}_{N_r}. \end{aligned} \quad (41)$$

To calculate (40), we first focus on an upper bound for the rate loss, as did in [8] for the limited feedback system. This will give a lower bound for (40) and provide useful insights. Then for a 2-user special case, we will provide asymptotic results which are accurate to get the mode switching points.

The following theorem provides an upper bound for the rate loss of the BD system with delay.

Theorem 6: Compared to the system with perfect CSIT, the rate loss for the u -th user of the delayed BD system is upper bounded by

$$\Delta R_{BD,u}^{(D)} = R_{BD,u} - R_{BD,u}^{(D)} \leq N_r \log_2 \left[(N_t - N_r) \frac{\gamma}{N_t} \epsilon_{e,u}^2 + 1 \right]. \quad (42)$$

Proof: See Appendix C. ■

Remark 6: This result is similar to the one in *Theorem 2* for the ZF system. The rate loss for each user is proportional to the number of receive antennas, which equals the number of data streams, so the user with more data streams will have a larger rate loss. There is a scaling factor $N_t - N_r$ on $\epsilon_{e,u}^2$, which is the number of interfering data streams. Equivalently, there are $N_t - N_r$ *virtual interfering single-antenna users* with the equivalent SNR as $\frac{\gamma}{N_t} \epsilon_{e,u}^2$. Therefore, the rate loss for each data stream of BD is lower than that of ZF, as BD has fewer virtual interfering users (see Table II), which means BD is more robust to the CSI delay. Intuitively, this is because the receiver of the BD system can perform joint decoding and there is no interference between data streams for the same user.

Next, we consider a two-user BD system and provide asymptotic results for the achievable rate. Without loss of generality, we focus on user 1. We denote γ_1 and γ_2 as SNRs for user 1 and user 2, and $N_{r,1}$ and $N_{r,2}$ as the numbers of receive antennas for user 1 and user 2.

Theorem 7: For a 2-user BD system with CSI delay, the achievable rate per receive antenna for user 1 is

$$\frac{R_{BD,1}^{(D)}}{N_{r,1}} = \frac{N_{r,2}}{N_{r,1}} \log_2 \left(\frac{\frac{N_{r,2}}{N_{r,1}} + \eta_1 \gamma_2 \epsilon_{e,1}^2}{\frac{N_{r,2}}{N_{r,1}} + \eta_2 \gamma_2 \epsilon_{e,1}^2} \right) + \log_2 (1 + \eta_1 \gamma_1) + \log_2 \frac{\eta_2}{\eta_1} + (\eta_1 - \eta_2) \log_2(e), \quad (43)$$

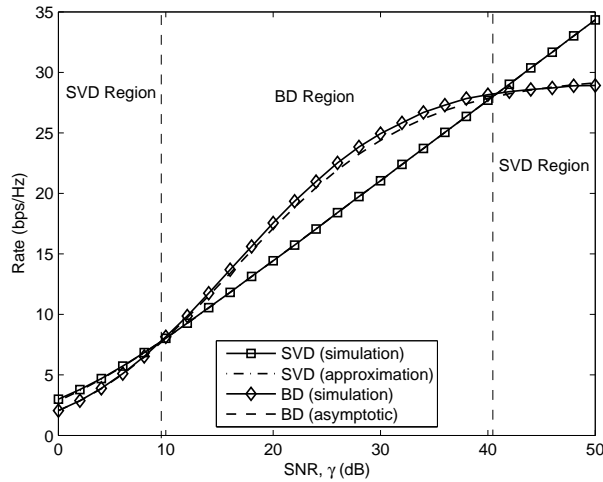


Fig. 7. Switching points between SVD and BD modes with CSI delay, $N_t = 4$, $f_c = 2$ GHz, $\tau = 0.001$ sec, and terminal speed is 10 km/hr.

with η_1 and η_2 as the positive solutions to

$$\eta_1 + \frac{\gamma_1 \eta_1}{\gamma_1 \eta_1 + 1} + \frac{N_{r,2}}{N_{r,1}} \frac{\gamma_2 \eta_1 \epsilon_{e,1}^2}{\eta_1 \gamma_2 \epsilon_{e,1}^2 + \frac{N_{r,2}}{N_{r,1}}} = 1, \quad \eta_2 + \frac{N_{r,2}}{N_{r,1}} \frac{\gamma_2 \eta_2 \epsilon_{e,1}^2}{\eta_2 \gamma_2 \epsilon_{e,1}^2 + \frac{N_{r,2}}{N_{r,1}}} = 1.$$

Proof: See Appendix D. ■

Such asymptotic results can be used to accurately predict the mode switching point.

3) *Mode Switching Point:* An example of mode switching for SVD and BD systems is shown in Fig. 7. We see that the asymptotic result from *Theorem 7* is also useful in the non-asymptotic region. Similar to $N_r = 1$, there are two switching points. Due to delay the SVD mode is preferred at both low and high SNR. Note that to keep a roughly same operating region for the MU mode, we have $v = 10$ km/hr for Fig. 7 compared to $v = 20$ km/hr in Fig. 2, which means the for the same delay the operating region for ZF (for $N_r = 1$) is larger than BD (for $N_r > 1$).

The operating region for different delays is plotted in Fig. 8. We can get similar observations as for the case of $N_r = 1$. In addition, compared to Fig. 3, we see that the BD operating region is smaller than ZF. Specifically, for BD to be active, we require $f_d \tau < 0.046$ and $\text{SNR} > 9.6$ dB. This is consistent with the observation from Fig. 7.

C. FDD System—CSI Delay and Channel Quantization

1) *SVD Transceiver:* For SVD transceiver of the FDD system, the receiver will feed back the index of a precoding matrix to the transmitter. Given $\mathbf{H}[n]$ and the precoding matrix $\mathbf{F}[n]$, the mutual information

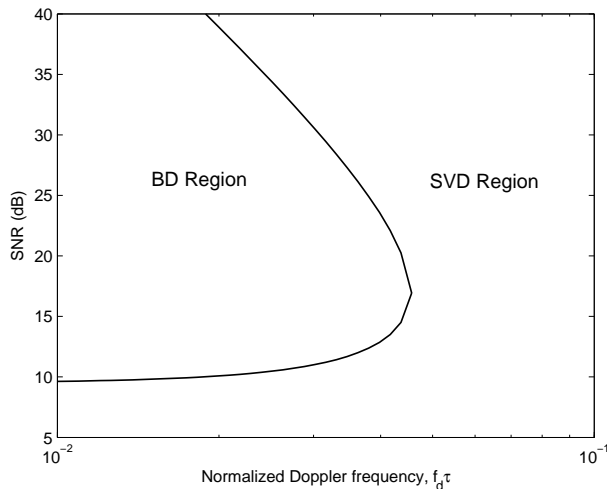


Fig. 8. Operating regions for SVD and BD with different CSI delays, $N_t = 4$, $N_r = 2$.

is

$$I(\mathbf{F}) = \log_2 \det \left(\mathbf{I}_{N_r} + \frac{\gamma}{N_r} \mathbf{H}[n] \mathbf{F}[n] \mathbf{F}^*[n] \mathbf{H}^*[n] \right). \quad (44)$$

Let $\bar{\mathbf{V}}_R[n]$ denote the first N_r columns of $\mathbf{V}[n]$, which is the right singular matrix of $\mathbf{H}[n]$. As shown in [46], the unitary precoding matrix that maximizes the mutual information $I(\mathbf{F})$ is $\mathbf{F}_{opt} = \bar{\mathbf{V}}[n]$.

With CSI delay, the available precoding matrix, $\hat{\mathbf{F}}[n]$, at the transmitter is based on $\mathbf{H}[n - D]$. The achievable rate of this system is

$$R_{SVD}^{(QD)} = \mathbb{E} \left[\log \det \left(\mathbf{I}_{N_r} + \mathbf{H}[n] \hat{\mathbf{F}}[n] \hat{\mathbf{F}}^*[n] \mathbf{H}^*[n] \right) \right]. \quad (45)$$

This is difficult to calculate. Similar to the delayed system, we will approximate (45) with (34), the capacity with perfect CSIT, which will be verified by numerical results.

2) *BD System*: For the BD system with both CSI delay and channel quantization, the feedback information is the quantization of the channel direction matrix, $\hat{\mathbf{H}}_u[n]$. Therefore, BD precoding matrices are designed based on $\hat{\mathbf{H}}_u[n - D]$, which achieves $\hat{\mathbf{H}}_u[n - D] \mathbf{T}_{u'}^{(QD)}[n] = \mathbf{0}$, $\forall u' \neq u$.

The achievable rate for the u -th user is given by

$$R_{BD,u}^{(QD)} = \mathbb{E} \left[\log_2 \det \left(\mathbf{I}_{N_r} + \frac{\gamma}{N_t} \mathbf{H}_{eff,u}[n] \mathbf{H}_{eff,u}^*[n] \hat{\mathbf{R}}_u^{-1}[n] \right) \right], \quad (46)$$

where $\hat{\mathbf{R}}_u[n]$ is given by

$$\hat{\mathbf{R}}_u[n] = \mathbf{H}_u[n] \left[\sum_{u' \neq u} \frac{\gamma}{N_t} \mathbf{T}_{u'}^{(QD)}[n] \mathbf{T}_{u'}^{(QD)*}[n] \right] \mathbf{H}_u^*[n] + \mathbf{I}_{N_r}. \quad (47)$$

The rate loss for such a system is given in the following theorem.

Theorem 8: With both CSI delay and channel quantization, the rate loss for the u -th user of the BD system is given by

$$\Delta R_{BD,u}^{(QD)} = R_{BD,u} - R_{BD,u}^{(QD)} \leq N_r \log_2 \left[(N_t - N_r) \frac{\gamma}{N_t} \left(\rho_u^2 \frac{N_t}{N_t - N_r} \cdot \frac{\bar{D}}{N_r} + \epsilon_{e,u}^2 \right) + 1 \right]. \quad (48)$$

where \bar{D} is the distortion of channel quantization, defined in (7).

Proof: See Appendix E. ■

Remark 7: *Theorem 8* explicitly shows the impact of quantization and delay on the BD system, through the terms of \bar{D} and $\epsilon_{e,u}^2$, respectively. Equivalently, there are $N_t - N_r$ virtual interfering single-antenna users with the equivalent SNR as $\frac{\gamma}{N_t} \left(\rho_u^2 \frac{N_t}{N_t - N_r} \cdot \frac{\bar{D}}{N_r} + \epsilon_{e,u}^2 \right)$. With a fixed codebook size or delay, the system is interference-limited.

3) *Mode Switching Point:* For BD with both delay and quantization, a lower bound of the achievable rate is provided in *Theorem 8*, but such a lower bound based on rate loss analysis is very loose. Analogous to the bound in (31) for the ZF system, we provide the following lower bound to calculate the mode switching point

$$R_{BD,u}^{(QD)} \geq \mathbb{E} \left[\log_2 \det \left(\mathbf{I}_{N_r} + \frac{\gamma}{\Delta_{BD,u}^{(QD)} N_t} \mathbf{H}_{eff,u}[n] \mathbf{H}_{eff,u}^*[n] \right) \right], \quad (49)$$

where $\Delta_{BD,u}^{(QD)} = \left[\left(\frac{\rho_u^2 \bar{D}}{N_r} + \frac{N_t - N_r}{N_t} \epsilon_{e,u}^2 \right) \gamma + 1 \right]$ is from *Theorem 8*. Essentially, this is to approximate $\hat{\mathbf{R}}_u[n]$ by $\Delta_{BD,u}^{(QD)} \mathbf{I}_{N_r}$, i.e. to approximate inter-user interference as white Gaussian noise. This lower bound can be calculated with the asymptotic result in *Theorem 5*.

Fig. 9 shows an example of the achievable rates for SVD and BD systems with both delay and quantization. Note that the mobility is very low ($v = 1$ km/hr), and the codebook size is large ($B = 18$), but BD can not outperform SVD over the whole SNR range, while the performance of SVD is very close to the case with perfect CSIT. It is also shown that the approximation (49) can be used to predict the mode switching point, while the lower bound from *Theorem 8* is very loose. The approximation for SVD is very accurate.

The operating regions for SVD and BD modes are plotted in Fig. 10. Compared with Fig. 5, we see that the operating region for BD is much smaller than ZF. This is because that the SVD system provides both spatial multiplexing gain and power gain, so its operating region is relative large. From Fig. 10(a), with a large codebook size $B = 30$, for BD to be active we need $f_d \tau < 0.023$. From Fig. 10(b), with a lower mobility $v = 3$ km/hr, we need codebook size $B > 22$ to get BD mode active. Therefore, we

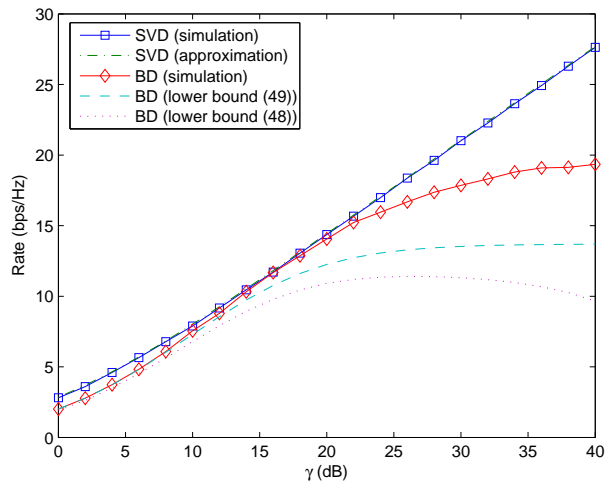


Fig. 9. Mode switching between SVD and BD modes with both CSI delay and channel quantization, $B = 18$, $N_t = 4$, $f_c = 2$ GHz, $\tau = 0.001$ sec, $v = 1$ km/hr.

would expect that in most of the practical scenarios with $N_r > 1$ the system will operate in the SVD mode.

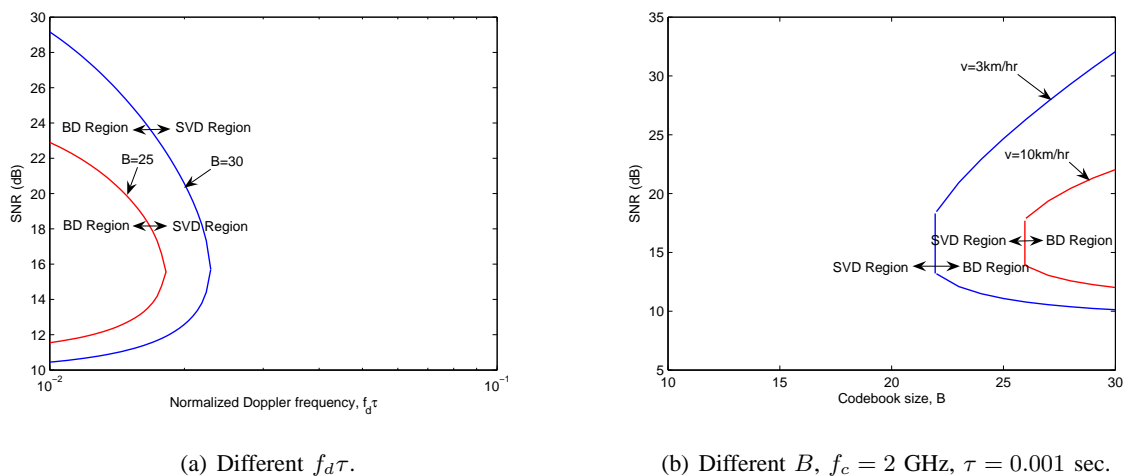


Fig. 10. Operating regions for SVD and BD with both CSI delay and quantization, $N_t = 4$.

V. CONCLUSION

We have derived the achievable ergodic rates of SU and MU-MIMO systems with imperfect CSIT, due to delay and channel quantization. It is shown that SU-MIMO is relatively more robust to imperfect CSIT.

For MU-MIMO, there are equivalently a number of virtual interfering users due to residual interference with CSI error, which makes the system interference-limited. A mode switching algorithm between SU and MU modes is proposed to improve the spectral efficiency. Mode switching points are calculated, which is based on the average SNR, normalized Doppler frequency, and the codebook size. With a fixed delay and codebook size, MU mode is only possible to be active in the medium SNR regime. When delay is large or the codebook size is small the MU mode may never be activated.

For future work, the MU-MIMO mode studied in this paper is designed with zero-forcing criterion, which is shown to be very sensitive to channel imperfection, so robust precoding design is needed. As power control is an effective way to combat interference, it is interesting to consider the efficient power control algorithm rather than equal power allocation to improve the performance. It is also important to extend to the system with a large number of users, where user scheduling considering imperfect channel information is required.

APPENDIX

A. Proof of Theorem 1

The instantaneous received SNR for the BF system with delay is $\gamma \left| \mathbf{h}^*[n] \mathbf{t}^{(D)}[n] \right|^2$, where $\mathbf{h}[n] = \rho \mathbf{h}[n-D] + \mathbf{e}[n]$ and $\mathbf{t}^{(D)}[n] = \tilde{\mathbf{h}}[n-D]$. The average SNR is

$$\begin{aligned}
 \overline{\text{SNR}}_{BF}^{(D)} &= \mathbb{E} \left[\gamma \left| \mathbf{h}^*[n] \mathbf{t}^{(D)}[n] \right|^2 \right] \\
 &= \gamma \mathbb{E} \left[\left| (\rho \mathbf{h}[n-D] + \mathbf{e}[n])^* \tilde{\mathbf{h}}[n-D] \right|^2 \right] \\
 &\stackrel{(a)}{=} \gamma \mathbb{E} [\rho^2 \|\mathbf{h}[n-D]\|^2] + \gamma \mathbb{E} [|\mathbf{e}^*[n] \tilde{\mathbf{h}}[n-D]|^2] \\
 &= \gamma \rho^2 N_t + \gamma \mathbb{E} \left[|\tilde{\mathbf{h}}^*[n-D] \cdot \mathbb{E}[\mathbf{e}[n] \mathbf{e}^*[n]] \cdot \tilde{\mathbf{h}}[n-D]| \right] \\
 &\stackrel{(b)}{=} \gamma \rho^2 N_t + \gamma \epsilon_e^2 \mathbb{E} \left[|\tilde{\mathbf{h}}^*[n-D] \tilde{\mathbf{h}}[n-D]| \right] \\
 &= \gamma (\rho^2 N_t + \epsilon_e^2).
 \end{aligned}$$

As $\mathbf{e}[n]$ is independent of $\mathbf{h}[n-D]$, it is also independent of $\tilde{\mathbf{h}}[n-D]$, which gives (a). Step (b) follows the fact that $\mathbf{e}[n] \sim \mathcal{CN}(\mathbf{0}, \epsilon_e^2 \mathbf{I}_{N_t})$.

B. Proof of Theorem 4

The noise plus interference for the ZF system with both channel quantization and delay is

$$\begin{aligned}
\Delta_{ZF,u}^{(QD)} &= \mathbb{E} \left[1 + \frac{\gamma}{U} \sum_{u' \neq u} \left| \mathbf{h}_u^*[n] \mathbf{t}_{u'}^{(QD)}[n] \right|^2 \right] \\
&= 1 + \frac{\gamma}{U} \mathbb{E} \left[\sum_{u' \neq u} \left| [\rho_u \mathbf{h}_u[n-D] + \mathbf{e}_u[n]]^* \mathbf{t}_{u'}^{(QD)}[n] \right|^2 \right] \\
&\stackrel{(a)}{=} 1 + \frac{\gamma}{U} \rho_u^2 \mathbb{E} \left[\sum_{u' \neq u} \left| \mathbf{h}_u^*[n-D] \mathbf{t}_{u'}^{(QD)}[n] \right|^2 \right] + \frac{\gamma}{U} \mathbb{E} \left[\sum_{u' \neq u} \left| \mathbf{e}_u^*[n] \mathbf{t}_{u'}^{(QD)}[n] \right|^2 \right] \\
&\stackrel{(b)}{=} 1 + \gamma \rho_u^2 2^{-\frac{B}{N_t-1}} + (U-1) \frac{\gamma}{U} \epsilon_{e,u}^2,
\end{aligned}$$

where (a) follows the independence between $\mathbf{h}_u[n-D]$ and $\mathbf{e}_u[n]$, and (b) follows (27) and *Theorem 2*.

C. Proof of Theorem 6

The achievable rate for the u -th user of BD system with perfect CSIT, $R_{BD,u}$, is given in (37). The rate with delay, $R_{BD,u}^{(D)}$, is given in (40), so the rate loss due to delay is

$$\begin{aligned}
\Delta R_{BD,u}^{(D)} &= R_{BD,u} - R_{BD,u}^{(D)} \\
&= \mathbb{E} \left[\log_2 \det \left(\mathbf{I}_{N_r} + \frac{\gamma}{N_t} \mathbf{H}_{eff,u}[n] \mathbf{H}_{eff,u}^*[n] \right) \right] \\
&\quad - \mathbb{E} \left[\log_2 \det \left(\mathbf{R}_u[n] + \frac{\gamma}{N_t} \mathbf{H}_{eff,u}[n] \mathbf{H}_{eff,u}^*[n] \right) \right] + \mathbb{E} [\log_2 \det \mathbf{R}_u[n]] \\
&\stackrel{(a)}{\leq} \mathbb{E} [\log_2 \det \mathbf{R}_u[n]] \\
&= \mathbb{E} \left\{ \log_2 \det \left[\mathbf{E}_u[n] \left(\sum_{u' \neq u} \frac{\gamma}{N_t} \mathbf{T}_{u'}^{(D)}[n] \mathbf{T}_{u'}^{(D)*}[n] \right) \mathbf{E}_u^*[n] + \mathbf{I}_{N_r} \right] \right\} \\
&\stackrel{(b)}{\leq} \log_2 \det \left\{ \mathbb{E} \left[\mathbf{E}_u[n] \left(\sum_{u' \neq u} \frac{\gamma}{N_t} \mathbf{T}_{u'}^{(D)}[n] \mathbf{T}_{u'}^{(D)*}[n] \right) \mathbf{E}_u^*[n] \right] + \mathbf{I}_{N_r} \right\} \\
&= \log_2 \det \left\{ \frac{\gamma}{N_t} (U-1) \mathbb{E} \left[\mathbf{E}_u[n] \mathbf{T}_{u'}^{(D)}[n] \mathbf{T}_{u'}^{(D)*}[n] \mathbf{E}_u^*[n] \right] + \mathbf{I}_{N_r} \right\} \\
&\stackrel{(c)}{=} \log_2 \det \left[\frac{\gamma}{N_t} (U-1) \epsilon_{e,u}^2 N_r \mathbf{I}_{N_r} + \mathbf{I}_{N_r} \right] \tag{50} \\
&= N_r \log_2 \left[(N_t - N_r) \frac{\gamma}{N_t} \epsilon_{e,u}^2 + 1 \right].
\end{aligned}$$

The inequality (a) follows from neglecting part of the positive semi-definite matrix of $\mathbf{R}_u[n]$ from the second term of the previous line, and (b) follows Jensen's inequality. As $\mathbf{E}_u[n]$ is a complex Gaussian

matrix and $\mathbf{T}_{u'}^{(D)}[n]$ is a unitary matrix, $\mathbf{E}_u[n]\mathbf{T}_{u'}^{(D)}[n]$ is also a Gaussian matrix with each entry having zero mean and variance $\epsilon_{e,u}^2$, which results (c).

D. Proof of Theorem 7

The interference-plus-noise covariance matrix for user 1 is

$$\mathbf{R}_1[n] = \frac{\gamma_2}{N_{r,2}} \mathbf{E}_1[n] \mathbf{T}_2^{(D)}[n] \mathbf{T}_2^{(D)*}[n] \mathbf{E}_1^*[n] + \mathbf{I}_{N_{r,1}} = \frac{\gamma_2}{N_{r,2}} \mathbf{E}_{eff,1}[n] \mathbf{E}_{eff,1}^*[n] + \mathbf{I}_{N_{r,1}}.$$

As $\mathbf{T}_2[n]$ is a unitary matrix independent of $\mathbf{E}_1[n]$, $\mathbf{E}_{eff,1}[n] = \mathbf{E}_1[n] \mathbf{T}_2^{(D)}[n]$ is a zero-mean complex Gaussian matrix, $\mathbf{E}_{eff,1} \sim \mathcal{CN}(\mathbf{0}_{N_{r,1} \times N_{r,2}}, N_{r,2} \epsilon_{e,1}^2 \mathbf{I}_{N_{r,1}})$.

The achievable rate for user 1 is

$$\begin{aligned} R_{BD,1}^{(D)} &= \mathbb{E} \left\{ \log_2 \det \left(\mathbf{I}_{N_{r,1}} + \frac{\gamma_1}{N_{r,1}} \mathbf{H}_{eff,1}[n] \mathbf{H}_{eff,1}^*[n] \left(\frac{\gamma_2}{N_{r,2}} \mathbf{E}_{eff,1}[n] \mathbf{E}_{eff,1}^*[n] + \mathbf{I}_{N_{r,1}} \right)^{-1} \right) \right\} \\ &= \mathbb{E} \left\{ \log_2 \det \left(\mathbf{I}_{N_{r,1}} + \frac{\gamma_1}{N_{r,1}} \mathbf{H}_{eff,1}[n] \mathbf{H}_{eff,1}^*[n] + \frac{\gamma_2}{N_{r,2}} \mathbf{E}_{eff,1}[n] \mathbf{E}_{eff,1}^*[n] \right) \right. \\ &\quad \left. - \log_2 \det \left(\mathbf{I}_{N_{r,1}} + \frac{\gamma_2}{N_{r,2}} \mathbf{E}_{eff,1}[n] \mathbf{E}_{eff,1}^*[n] \right) \right\}. \end{aligned}$$

Denote $\mathbf{H}_{w,1}$ and $\mathbf{H}_{w,2}$ as $N_{r,1} \times N_{r,1}$ and $N_{r,1} \times N_{r,2}$ Gaussian matrices with entries having zero mean and unit variance. Statistically equivalently, we have

$$\begin{aligned} R_{BD,1}^{(D)} &= \mathbb{E} \left\{ \log_2 \det \left(\mathbf{I}_{N_{r,1}} + [\mathbf{H}_{w,1} \ \mathbf{H}_{w,2}] \begin{bmatrix} \frac{\gamma_1}{N_{r,1}} \mathbf{I}_{N_{r,1}} & \mathbf{0} \\ \mathbf{0} & \frac{\gamma_2 \epsilon_{e,1}^2}{N_{r,2}} \mathbf{I}_{N_{r,2}} \end{bmatrix} [\mathbf{H}_{w,1} \ \mathbf{H}_{w,2}]^* \right) \right. \\ &\quad \left. - \log_2 \det \left(\mathbf{I}_{N_{r,1}} + \frac{\gamma_2 \epsilon_{e,1}^2}{N_{r,2}} \mathbf{H}_{w,2} \mathbf{H}_{w,2}^* \right) \right\}. \end{aligned}$$

Denote the first term as $R_{1,1}$ and the second term as $R_{1,2}$. From [45], [47], the following asymptotic results can be derived

$$\begin{aligned} \frac{R_{1,1}}{N_{r,1}} &= \log_2(1 + \eta_1 \gamma_1) + \frac{N_{r,2}}{N_{r,1}} \log_2 \left(1 + \frac{N_{r,1}}{N_{r,2}} \eta_1 \gamma_2 \epsilon_{e,1}^2 \right) + \log_2 \frac{1}{\eta_1} + (\eta_1 - 1) \log_2(e), \\ \frac{R_{1,2}}{N_{r,1}} &= \frac{N_{r,2}}{N_{r,1}} \log_2 \left(1 + \frac{N_{r,1}}{N_{r,2}} \eta_2 \gamma_2 \epsilon_{e,1}^2 \right) + \log_2 \frac{1}{\eta_2} + (\eta_2 - 1) \log_2(e), \end{aligned}$$

where η_1 and η_2 are the positive solutions to

$$\eta_1 + \frac{\gamma_1 \eta_1}{\gamma_1 \eta_1 + 1} + \frac{N_{r,2}}{N_{r,1}} \frac{\gamma_2 \eta_1 \epsilon_{e,1}^2}{\eta_1 \gamma_2 \epsilon_{e,1}^2 + \frac{N_{r,2}}{N_{r,1}}} = 1, \quad \eta_2 + \frac{N_{r,2}}{N_{r,1}} \frac{\gamma_2 \eta_2 \epsilon_{e,1}^2}{\eta_2 \gamma_2 \epsilon_{e,1}^2 + \frac{N_{r,2}}{N_{r,1}}} = 1.$$

The achievable rate per receive antenna with CSI delay for user 1 is

$$\frac{R_{BD,1}^{(D)}}{N_{r,1}} = \frac{R_{1,1}}{N_{r,1}} + \frac{R_{1,2}}{N_{r,1}}.$$

E. Proof of Theorem 8

The achievable rate for the u -th user of BD system with perfect CSIT, $R_{BD,u}$, is given in (37). The rate with both channel quantization and delay, $R_{BD,u}^{(QD)}$, is given in (46). Therefore, the rate loss is

$$\begin{aligned}
\Delta R_{BD,u}^{(QD)} &= R_{BD,u} - R_{BD,u}^{(QD)} \\
&\stackrel{(a)}{\leq} \mathbb{E} \left[\log_2 \det \hat{\mathbf{R}}_u \right] \\
&\leq \log_2 \det \left\{ \mathbb{E} \left[\mathbf{H}_u[n] \left(\sum_{u' \neq u} \frac{\gamma}{N_t} \mathbf{T}_{u'}^{(QD)}[n] \mathbf{T}_{u'}^{(QD)*}[n] \right) \mathbf{H}_u[n]^* \right] + \mathbf{I}_{N_r} \right\} \\
&\stackrel{(b)}{=} \log_2 \det \left\{ \frac{\gamma}{N_t} (U-1) \left[\rho_u^2 \mathbb{E} \left(\mathbf{H}_u[n-D] \mathbf{T}_{u'}^{(QD)}[n] \mathbf{T}_{u'}^{(QD)*}[n] \mathbf{H}_u^*[n-D] \right) \right. \right. \\
&\quad \left. \left. + \mathbb{E} \left(\mathbf{E}_u[n] \mathbf{T}_{u'}^{(QD)}[n] \mathbf{T}_{u'}^{(QD)*}[n] \mathbf{E}_u^*[n] \right) \right] + \mathbf{I}_{N_r} \right\} \\
&\stackrel{(c)}{=} \log_2 \det \left[\frac{\gamma}{N_r} \rho_u^2 \bar{D} \mathbf{I}_{N_r} + \frac{\gamma}{N_t} (U-1) \epsilon_{e,u}^2 N_r \mathbf{I}_{N_r} + \mathbf{I}_{N_r} \right] \\
&= N_r \log_2 \left[(N_t - N_r) \frac{\gamma}{N_t} \left(\rho_u^2 \frac{N_t}{N_t - N_r} \cdot \frac{\bar{D}}{N_r} + \epsilon_{e,u}^2 \right) + 1 \right], \tag{51}
\end{aligned}$$

Step (a) follows the same argument in the proof in Appendix C, while step (b) follows the independence between $\mathbf{H}_u[n-D]$ and $\mathbf{E}_u[n]$. Step (c) follows (50) and the *Theorem 1* in [8].

REFERENCES

- [1] I. E. Telatar, "Capacity of multiantenna Gaussian channels," *Europ. Trans. Telecommun.*, vol. 10, pp. 585–595, Nov. 1999.
- [2] A. Goldsmith, S. A. Jafar, N. Jindal, and S. Vishwanath, "Capacity limits of MIMO channels," *IEEE J. Select. Areas Commun.*, vol. 51, no. 6, pp. 684–702, Jun. 2003.
- [3] D. Gesbert, M. Kountouris, R. W. Heath, Jr., C. B. Chae, and T. Salzer, "Shifting the MIMO paradigm: From single user to multiuser communications," *IEEE Signal Processing Magazine*, vol. 24, no. 5, pp. 36–46, Sept. 2007.
- [4] N. Jindal, "MIMO broadcast channels with finite rate feedback," *IEEE Trans. Inform. Theory*, vol. 52, no. 11, pp. 5045–5059, Nov. 2006.
- [5] T. Yoo, N. Jindal, and A. Goldsmith, "Multi-antenna downlink channels with limited feedback and user selection," *IEEE J. Select. Areas Commun.*, vol. 25, no. 7, pp. 1478–1491, Sept. 2007.
- [6] G. Caire, N. Jindal, M. Kobayashi, and N. Ravindran, "Multiuser MIMO downlink made practical: Achievable rates with simple channel state estimation and feedback schemes," *Submitted to IEEE Trans. Information Theory*, vol. Available online at <http://arxiv.org/abs/0711.2642>.
- [7] P. Ding, D. J. Love, and M. D. Zoltowski, "Multiple antenna broadcast channels with partial and limited feedback," *IEEE Trans. Signal Processing*, vol. 55, no. 7, pp. 3417–3428, Jul. 2007.
- [8] N. Ravindran and N. Jindal, "Limited feedback-based block diagonalization for the MIMO broadcast channel," *to appear, IEEE Journal Sel. Areas in Communications*, 2008.

- [9] K. Huang, R. W. Heath, Jr., and J. G. Andrews, "Space division multiple access with a sum feedback rate constraint," *IEEE Trans. Signal Processing*, vol. 55, no. 7, pp. 3879–3891, Jul. 2007.
- [10] A. Lapidoth, S. Shamai, and M. Wigger, "On the capacity of fading MIMO broadcast channels with imperfect transmitter side-information," in *Proceedings of the 43rd Allerton Conference on Communication, Control and Computing*.
- [11] A. Narula, M. J. Lopez, M. D. Trott, and G. W. Wornell, "Efficient use of side information in multiple-antenna data transmission over fading channels," *IEEE J. Select. Areas Commun.*, vol. 16, pp. 1423–1436, Oct. 1998.
- [12] D. J. Love, R. W. Heath, Jr., and T. Strohmer, "Grassmannian beamforming for multiple-input multiple-output wireless systems," *IEEE Trans. Inform. Theory*, vol. 49, no. 10, pp. 2735–2745, Oct. 2003.
- [13] K. Mukkavilli, A. Sabharwal, E. Erkip, and B. Aazhang, "On beamforming with finite rate feedback in multiple-antenna systems," *IEEE Trans. Inform. Theory*, vol. 49, no. 10, pp. 2562–2579, Oct. 2003.
- [14] D. J. Love, R. W. Heath, Jr., W. Santipach, and M. Honig, "What is the value of limited feedback for MIMO channels?" *IEEE Commun. Mag.*, vol. 42, no. 10, pp. 54–59, Oct. 2004.
- [15] T. Yoo and A. Goldsmith, "Capacity and power allocation for fading MIMO channels with channel estimation error," *IEEE Trans. Inform. Theory*, vol. 52, no. 5, pp. 2203–2214, May 2006.
- [16] M. Costa, "Writing on dirty paper," *IEEE Trans. Inform. Theory*, vol. 39, no. 3, pp. 439–441, May 1983.
- [17] W. Yu and J. Cioffi, "The sum capacity of a Gaussian vector broadcast channel," *IEEE Trans. Inform. Theory*, vol. 50, no. 9, pp. 1875–1892, Sep. 2004.
- [18] S. Vishwanath, N. Jindal, and A. Goldsmith, "Duality, achievable rates, and sum-rate capacity of MIMO broadcast channels," *IEEE Trans. Inform. Theory*, vol. 49, no. 10, pp. 2658–2668, Oct. 2003.
- [19] P. Viswanath and D. N. C. Tse, "Sum capacity of the vector Gaussian broadcast channel and uplink-downlink duality," *IEEE Trans. Inform. Theory*, vol. 49, no. 8, pp. 1912–1921, Aug. 2003.
- [20] H. Weingarten, Y. Steinberg, and S. Shamai, "The capacity region of the Gaussian multiple-input multiple-output broadcast channel," *IEEE Trans. Inform. Theory*, vol. 52, no. 9, pp. 3936–3964, Sept. 2006.
- [21] L. U. Choi and R. D. Murch, "A transmit preprocessing technique for multiuser MIMO systems using a decomposition approach," *IEEE Trans. Wireless Commun.*, vol. 3, no. 1, pp. 20–24, Jan. 2004.
- [22] Q. H. Spencer, A. L. Swindlehurst, and M. Haardt, "Zero-forcing methods for downlink spatial multiplexing in multi-user MIMO channels," *IEEE Trans. Signal Processing*, vol. 52, no. 2, pp. 461–471, Feb. 2004.
- [23] Z. Pan, K. K. Wong, and T. S. Ng, "Generalized multiuser orthogonal space-division multiplexing," *IEEE Trans. Wireless Commun.*, vol. 3, no. 6, pp. 1969–1973, Nov. 2004.
- [24] Z. Shen, R. Chen, J. G. Andrews, R. W. Heath, Jr., and B. L. Evans, "Sum capacity of multiuser MIMO broadcast channels with block diagonalization," *IEEE Trans. Wireless Commun.*, vol. 6, no. 6, pp. 2040–2045, Jun. 2007.
- [25] J. Lee and N. Jindal, "High SNR analysis for MIMO broadcast channels: Dirty paper coding vs. linear precoding," *IEEE Trans. Inform. Theory*, vol. 53, no. 12, pp. 4787–4792, Dec. 2007.
- [26] N. Ravindran, N. Jindal, and H. C. Huang, "Beamforming with finite rate feedback for LOS MIMO downlink channels," in *Proc. IEEE Globecom*, Washington, DC, Nov. 2007, pp. 4200–4204.
- [27] R. H. Clarke, "A statistical theory of mobile radio reception," *Bell System Tech. J.*, vol. 47, pp. 957–1000, 1968.
- [28] D. L. Goeckel, "Adaptive coding for time-varying channels using outdated fading estimates," *IEEE Trans. Commun.*, vol. 47, no. 6, pp. 844–855, Jun. 1999.
- [29] E. N. Onggosanusi, A. Gatherer, A. G. Dabak, and S. Hosur, "Performance analysis of closed-loop transmit diversity in the presence of feedback delay," *IEEE Trans. Commun.*, vol. 49, no. 9, pp. 1618–1630, Sept. 2001.

- [30] H. T. Nguyen, J. B. Anderson, and G. F. Pedersen, "Capacity and performance of MIMO systems under the impact of feedback delay," in *Proc. of the IEEE Int. Symp. on Personal Indoor and Mobile Radio Comm.*, Barcelona, Spain, Sept. 2004, pp. 53–57.
- [31] S. Zhou and G. B. Giannakis, "How accurate channel prediction needs to be for transmit-beamforming with adaptive modulation over Rayleigh MIMO channels," *IEEE Trans. Wireless Commun.*, vol. 3, no. 4, pp. 1285–1294, Jul. 2004.
- [32] W. Santipach and M. Honig, "Asymptotic capacity of beamforming with limited feedback," in *Proc. IEEE Int. Symp. Information Theory*, Chicago, IL, Jun./Jul. 2004, p. 290.
- [33] J. H. Conway, R. H. Hardin, and N. J. A. Sloane, "Packing lines, planes, etc.: Packings in Grassmannian space," *Expr. Math.*, vol. 5, pp. 139–159, 1996.
- [34] W. Dai, Y. Liu, and B. Rider, "Quantization bounds on Grassmann manifolds and applications in MIMO systems," *IEEE Trans. Inform. Theory*, vol. 54, no. 3, pp. 1108–1123, Mar. 2008.
- [35] A. Goldsmith, *Wireless Communications*. Cambridge University Press, 2005.
- [36] M. Alouini and A. Goldsmith, "Capacity of Rayleigh fading channels under different adaptive transmission and diversity-combining techniques," *IEEE Trans. Veh. Technol.*, vol. 48, no. 4, pp. 1165–1181, Jul. 1999.
- [37] M. Médard, "The effect upon channel capacity in wireless communications of perfect and imperfect knowledge of the channel," *IEEE Trans. Inform. Theory*, vol. 46, pp. 933–946, May 2000.
- [38] B. Hassibi and B. M. Hochwald, "How much training is needed in multiple-antenna wireless links?" *IEEE Trans. Inform. Theory*, vol. 49, pp. 951–963, Apr. 2003.
- [39] A. M. Tulino and S. Verdú, "Random matrix theory and wireless communications," *Found. Trends Commun. Inf. Theory*, vol. 1, no. 1, 2004.
- [40] E. Biglieri, A. M. Tulino, and G. Taricco, "How far away is infinity? Using asymptotic analyses in multiple antenna systems," in *Proc. IEEE Int. Symp. on Spread Spectrum Tech. and Applications (ISSSTA '02)*, Sep. 2002, pp. 1–6.
- [41] A. M. Tulino, A. Lozano, and S. Verdú, "MIMO capacity with channel state information at the transmitter," in *Proc. IEEE Int. Symp. on Spread Spectrum Tech. and Applications (ISSSTA '04)*, Aug. 2004.
- [42] D. Tse and P. Viswanath, *Fundamentals of Wireless Communication*. Cambridge University Press, 2005.
- [43] S. Verdú and S. Shamai (Shitz), "Spectral efficiency of CDMA with random spreading," *IEEE Trans. Inform. Theory*, vol. 45, no. 3, pp. 622–640, Mar. 1999.
- [44] P. Rapajic and D. Popescu, "Information capacity of a random signature multiple-input multiple-output channel," *IEEE Trans. Commun.*, vol. 48, pp. 1245–1248, Aug. 2000.
- [45] S. Shim, J. S. Kwak, R. W. Heath, Jr., and J. G. Andrews, "Block diagonalization for multi-user MIMO with other-cell interference," *IEEE Trans. Wireless Commun.*, to appear.
- [46] D. J. Love and R. W. Heath, Jr., "Limited feedback unitary precoding for spatial multiplexing systems," *IEEE Trans. Inform. Theory*, vol. 51, no. 8, pp. 2967–2976, Aug. 2005.
- [47] A. Lozano and A. M. Tulino, "Capacity of multiple-transmit multiple-receive antenna architectures," *IEEE Trans. Inform. Theory*, vol. 48, no. 12, pp. 3117–3129, Dec. 2002.